Available online at www.sciencedirect.com
SCIENCE DIRECT®
Physics Letters B 614 (2005) 143–154
PHYSICS LETTERS B
www.elsevier.com/locate/physletb

Supersymmetric dark matter search via spin-dependent interaction with ^{3}He

E. Moulin, F. Mayet, D. Santos

Laboratoire de Physique Subatomique et de Cosmologie, CNRS/IN2P3 et Université Joseph Fourier, 53, avenue des Martyrs, 38026 Grenoble cedex, France

Received 16 February 2005; received in revised form 21 March 2005; accepted 29 March 2005

Available online 8 April 2005

Editor: L. Rolandi

Abstract

The potentialities of MIMAC-He3, a MIcro-tpc MAtrix of Chambers of Helium-3, for supersymmetric dark matter search are discussed within the framework of effective MSSM models without gaugino mass unification at the GUT scale. A phenomenological study has been done to investigate the sensitivity of the MIMAC-He3 detector to neutralinos ($M_{\tilde{\chi}} \gtrsim 6\,\mathrm{GeV}/c^2$) via spin-dependent interaction with ^{3}He as well as its complementarity to direct and indirect detection experiments. Comparison with other direct dark matter searches will be presented in a WIMP model-independent framework.

PACS: 95.35; 67.57; 07.57.K; 11.30.P

Keywords: Dark matter; Supersymmetry; Helium-3; Spin-dependent interaction

1. Introduction

Since recent high accuracy experimental results in observational cosmology, the existence of non-baryonic dark matter seems to be well established. CMB results [1,2] used in combination with high redshift supernova [3] and large scale structure surveys [4], seem to point out that most of the matter in the Universe consists of cold non-baryonic dark matter (CDM). As a consequence, the range for CDM density has reached an unprecedented level of accuracy: $\Omega_{\mathrm{CDM}}h_0^2 = 0.12 \pm 0.04$ [1], with $h_0 = 0.73 \pm 0.03$ the normalized Hubble expansion rate [5]. This non-baryonic cold dark matter consists of still not detected particles whose well-motivated candidates are the WIMPs (weakly interacting massive particles). Supersymmetric theories with R-parity conservation provide a suitable candidate, the lightest supersymmetric particle (LSP), which can significantly account for CDM [6]. In various SUSY scenarii, this neutral and colorless particle is the lightest neutralino $\tilde{\chi}$.

E-mail address: emmanuel.moulin@lpsc.in2p3.fr (E. Moulin).

0370-2693
doi:10.1016/j.physletb.2005.03.068

Tremendous experimental efforts on a host of techniques have been made in the field of direct search of non-baryonic dark matter [7–10]. Several detectors reached sufficient sensitivity to begin to test regions of the SUSY parameter space. However, they are still limited by neutron interactions in the sensitive medium. Energy threshold effect combined with the use of a heavy target nucleus leads to significant sensitivity loss for light WIMPs.

The main purpose of this Letter is to show the interest to perform an experimental effort as MIMAC-He3 (MIcro-tpc MAtrix of Chambers of Helium-3) [11,12] in order to search for non-baryonic dark matter particles, within the framework of effective MSSM models without gaugino unification at GUT scale. A full estimation of the neutralino $\tilde{\chi}$ detection rate in MIMAC-He3 has been performed including the computation of the spin-dependent cross-section on ^{3}He. An emphasis on light neutralino sensitivity of MIMAC-He3 will be laid as well as its complementarity with scalar and indirect detections. A comparison to other spin-dependent dark matter experiments will be shown in a WIMP model-independent framework.

2. ^{3}He as sensitive medium for dark matter search

As reported elsewhere [13–15], the use of ^{3}He is motivated by its privileged features for dark matter search compared with other target nuclei. With ^{3}He being a spin 1/2 nucleus, a detector made of such a material will be sensitive to the spin-dependent interaction, leading to a natural complementarity to existing detectors mainly sensitive to the spin-independent interaction. For massive WIMPs, the maximum recoil energy depends very weakly on the WIMP mass as the ^{3}He nucleus is much lighter ($m(^3\text{He}) = 2.81\ \text{GeV}/c^2$). Therefore, the energy range in which all the sought events fall is $\lesssim 6$ keV. Thus, the recoil energy range needs to be studied from energy threshold up to 6 keV. This narrow range, for the searched events, represents a key point to discriminate these rare events from the background. The ^{3}He presents in addition the following advantages with respect to other sensitive materials for WIMPs detection:

- a very low Compton cross-section to gamma rays, two orders of magnitude weaker than in Ge: 9×10^{-1} barns for 10 keV γ-rays compared to 2×10^2 barns in Ge;
- no intrinsic X-rays;
- the neutron signature. The capture process $n + {}^3\text{He} \rightarrow p + {}^3\text{H} + 764$ keV gives very different signals with respect to the WIMP events.

This property is a key point for dark matter search as neutrons in underground laboratory are considered as the ultimate background. Careful simulations and measurements of the neutron production induced by high energy cosmic muon interaction in the shielding are compulsory [12,16]. Despite this, any dark matter detector should be able to separate a $\tilde{\chi}$ event from the neutron background. Using energy measurement and electron-recoil discrimination, MIMAC-He3 presents a high rejection for neutrons due to capture and multi-scattering of neutrons [12]. A detailed description of the MIMAC-He3 project can be found in a forthcoming paper [12].

3. Theoretical framework

The potentiality of such a detector has been investigated in the framework of effective MSSM (minimal supersymmetric models) with no gaugino mass unification at GUT scale, thus extending LEP-allowed $\tilde{\chi}$ mass range. This work follows early SUSY calculations in [17], done with a model-dependent analysis within restrictive MSSM.

3.1. Effective MSSM with no gaugino mass unification

The lightest neutralino $\tilde{\chi}$ is a well-motivated candidate as it corresponds to the LSP in many SUSY models [6]. It is defined as the lowest mass linear combination of the supersymmetric partners of the U(1) and SU(2) gauge bosons, the bino $\tilde{B}$, the wino $\tilde{W}$, and the two higgsinos $\tilde{H}_1^0$, $\tilde{H}_2^0$:

$$\tilde{\chi} = a\tilde{B} + b\tilde{W} + c\tilde{H}_1^0 + d\tilde{H}_2^0. \tag{1}$$

A standard assumption of supersymmetric models is the unification condition of the three gaugino masses M_i $(i = 1, 2, 3)$ at the GUT scale ($\sim 2 \times 10^{16}$ GeV). This hypothesis implies at the electroweak scale (EW) the following relation between M_1 and M_2: $M_1 =$

$5/3\tan^2\theta_W M_2$, yielding the standard formula $M_1 \simeq 0.5M_2$ at the EW scale. Under the unification condition, the lower bound on the lightest neutralino mass is found to be $M_{\tilde{\chi}} \geqslant 36\ \mathrm{GeV}/c^2$ derived from LEP2 analysis [5]. In order to explore the probable existence of lighter neutralinos, supersymmetric models where M_1 and M_2 are considered as independent parameters have been investigated [18]. The unification constraint can be relaxed by the introduction of a free parameter R defined by

$$M_1 \equiv RM_2. \tag{2}$$

Thus, the departure from the gaugino mass universality can be studied with $R < 0.5$ [19–21]. The neutralino $\tilde{\chi}$ can be lighter than the limit obtained in scenarii with gaugino mass unification [20]. In non-universal cases, the lower limit on the neutralino mass exists whatever the R value but diminishes when $R < 0.5$ becoming roughly $M_{\tilde{\chi}} \geqslant R \times M_{\chi^\pm}$. The lightest neutralinos are typically found in SUSY models associated with $M_1 \ll M_2, \mu$, where a significant higgsino fraction is required to obtain relatively high cross-sections.

3.2. SUSY parameter space

A minimal set of parameters has been used in the framework of an effective MSSM with no gaugino mass unification at GUT scale. The supersymmetric parameter space consists of the following independent parameters:

$$M_2,\ \mu,\ M_0,\ M_A,\ \tan\beta,\ A_{t,b},\ R$$

with M_2 the gaugino mass parameter, μ the higgsino mass parameter, M_0 the common scalar mass, M_A the pseudo-scalar Higgs mass, $\tan\beta$ the Higgs VEV ratio, $A_{t,b}$ the trilinear couplings and R the ratio characterizing the amount of non-universality. A large scan of the parameter space has been done with the DarkSUSY code [22] in which the departure from the universality has been implemented. This code is a numerical package for supersymmetric dark matter calculations including all resonances, thresholds and coannihilations for cross-sections. The ranges used for the scan on each parameter defined at electroweak (EW) scale are given in Table 1. The resulting scan corresponds to a total number of $\sim 25 \times 10^6$ models. It also includes the usual scheme with U(1) and SU(2) gaugino mass unification at GUT scale, for which $R = 0.5$ at the EW scale.

Table 1
Scan of the SUSY parameter space including the departure from U(1) and SU(2) gaugino unification at GUT scale. The total number is $\sim 25 \times 10^6$ models

Parameter	Minimum	Maximum	Number of steps
M_0 (GeV)	100	1000	11
M_2 (GeV)	50	1000	20
M_A (GeV)	100	1000	10
$\lvert\mu\rvert$ (GeV)	50	1000	20
		$\mathrm{sign}(\mu) = \pm 1$	
$\tan\beta$	5	60	12
R	0.01	0.5	10
		$A_{t,b} = 0$	

3.3. Experimental constraints

3.3.1. Accelerator limits

Standard bounds from colliders usually come from derivations in mSUGRA type model analysis [5]. In the non-universal scheme, such constraints have to be redefined. All the limits given below are extracted from Ref. [5]. LEP and Tevatron set mass bounds on supersymmetric charged particles giving the lower limit for chargino masses: $M_{\chi^\pm} \gtrsim 103\ \mathrm{GeV}/c^2$. In models where the pseudoscalar mass is heavy, the limit obtained from LEP2 on the lightest CP even Higgs mass is $M_h \geqslant 114\ \mathrm{GeV}/c^2$. Nevertheless, in models with a light pseudoscalar ($M_A \leqslant 200\ \mathrm{GeV}/c^2$), the LEP2 constraint is relaxed and the absolute bound is $M_h \geqslant 91.6\ \mathrm{GeV}/c^2$. These constraints have been imposed to the SUSY models used for this study. For the $\tilde{\chi}$ mass, the commonly quoted and employed bound, $36\ \mathrm{GeV}/c^2$, is derived from the lower bound of the chargino mass $M_{\chi^\pm}$ determined at LEP2 under the assumption that the U(1) and SU(2) gaugino masses M_1 and M_2 satisfy the standard relationship $M_1 \simeq 0.5M_2$ at the EW scale. In such scenarii, it is only through the relation between the gaugino parameters M_1 and M_2 that the neutralino mass limit is obtained. Indeed, the lower bound on $M_{\chi^\pm}$ converts into bounds on M_2 and μ. The relationship between M_1 and M_2 implies a lower bound on M_1, leading to the commonly used limit on $M_{\tilde{\chi}}$. In non-universal case, an absolute lower limit on the $\tilde{\chi}$ mass cannot be obtained because the chargino and neutralino masses are uncorrelated

and the lower limit on the neutralino mass diminishes with $R < 0.5$. However, a lower limit can be derived from the cosmological bound on the amount of CDM, the latter being roughly inversely proportional to the square root of $M_{\tilde{\chi}}$ [20].

3.3.2. Indirect limits

In order to take into account latest results of observational cosmology [5], we required the SUSY models to yield a $\tilde{\chi}$ relic density $\Omega_{\tilde{\chi}}$ with a dominant contribution to dark matter. Only models giving a $\Omega_{\tilde{\chi}}$ in the following range are considered:

$$0.02 \leqslant \Omega_{\chi} h_0^2 \leqslant 0.15.$$

The relic density is constrained in such a range in order to account for various effects. First, it has been shown [23], that the uncertainty, for all SUSY codes, in the relic density calculation can be quite large. Indeed, mass differences of about 1% in the input SUSY mass spectrum, lead to a spread in the calculated densities of 10%. The discrepancies can be even larger for some SUSY parameter space region. Concerning the lower bound, it should be highlighted that one wants to keep models which provide a non-negligible relic density, that is to say neutralinos which can contribute significatively to the amount of CDM, but which not necessarily fill the entire amount of CDM. A lower bound on the $\tilde{\chi}$ mass can be derived from the upper bound on the $\tilde{\chi}$ relic density. It is estimated to be $M_{\tilde{\chi}} \gtrsim 6\ \mathrm{GeV}/c^2$ [20,21]. Experimental constraints from accelerators on the muon anomalous magnetic moment, $a_{\mu} \equiv (g_{\mu} - 2)/2$, and the $b \to s + \gamma$ decay are taken into account. For the muon anomalous magnetic moment, we choose a limit taking into account $e^- e^+$ and τ results [5]

$$-25 \leqslant a_{\mu} \times 10^{10} \leqslant 69.$$

As many contributions have to be clarified, our range is conservative. Concerning the branching ratio of the rare decay, $\mathrm{BR}(b \to s + \gamma)$, from CLEO, BELLE and ALEPH measurements [5], models are required to give a prediction falling in the range

$$2.04 \leqslant \mathrm{BR}(b \to s + \gamma) \times 10^4 \leqslant 4.42.$$

3.3.3. Astrophysical parameters

As far as the detection on Earth is concerned, a local halo model is required. A spherical isothermal distribution with standard galactic halo parameter have been used. The velocity distribution is assumed to be a standard isotropic Maxwellian distribution in the galactic frame with an average rms velocity v truncated above the escape velocity of the galaxy. We assume no clumpy structures in the halo even if studies have been done in such cases [24]. The set of astrophysical parameters, commonly used [5], for the SUSY parameter scan is

$$\rho_0 = 0.3\ \mathrm{GeV}/c\ \mathrm{cm}^{-3} \quad \text{and} \quad v = 220\ \mathrm{km/s}^{-1}.$$

4. Neutralino direct detection with ^{3}He

4.1. Spin-dependent cross-section on ^{3}He

The neutralino $\tilde{\chi}$ being a Majorana fermion, only the scalar (via H and h in t-channel and $\tilde{q}$ in s-channel) and the axial (via Z in t-channel and $\tilde{q}$ in s-channel) interactions remain, the first one being called spin-independent (SI) and the second one, the spin-dependent (SD) vanishing in the case of zero spin nuclei. ^{3}He being an spin 1/2 nucleus is sensitive to the axial interaction with the neutralino. Such an interaction is predominant on the scalar one for light nuclei such as ^{3}He [6]. The spin-dependent cross-section on ^{3}He has been evaluated in the whole parameter space using the DarkSUSY code [22]. The $\tilde{\chi}$-quark elastic scattering amplitude are calculated via $\tilde{q}$ or Z exchange. The amplitude on the nucleon is then evaluated by adding the contribution of each quark weighted by the quark content of the nucleon. In order to obtain the cross-section on the nucleus, we will use the tree level expansion. The expression at zero momentum transfer of the cross-section on ^{3}He is then estimated as

$$\sigma_{\mathrm{SD}}\left(^3\mathrm{He}\right) = \frac{32}{\pi} G_F^2 \mu^2 \frac{J+1}{J} \left(\langle S_p \rangle a_p + \langle S_n \rangle a_n\right)^2, \quad (3)$$

where G_F is the Fermi coupling constant, μ is the reduced mass of the ^{3}He–$\tilde{\chi}$ system, J the ground state angular momentum and $\langle S_{p,n} \rangle$ the proton and neutron spin content of ^{3}He. Using this expression, the $\tilde{\chi}$ event rate has been calculated for a 10 kg ^{3}He matrix and compared with the expected background rate. The result is presented on Fig. 1 for SUSY models not excluded by collider constraints (Section 3.3.1)

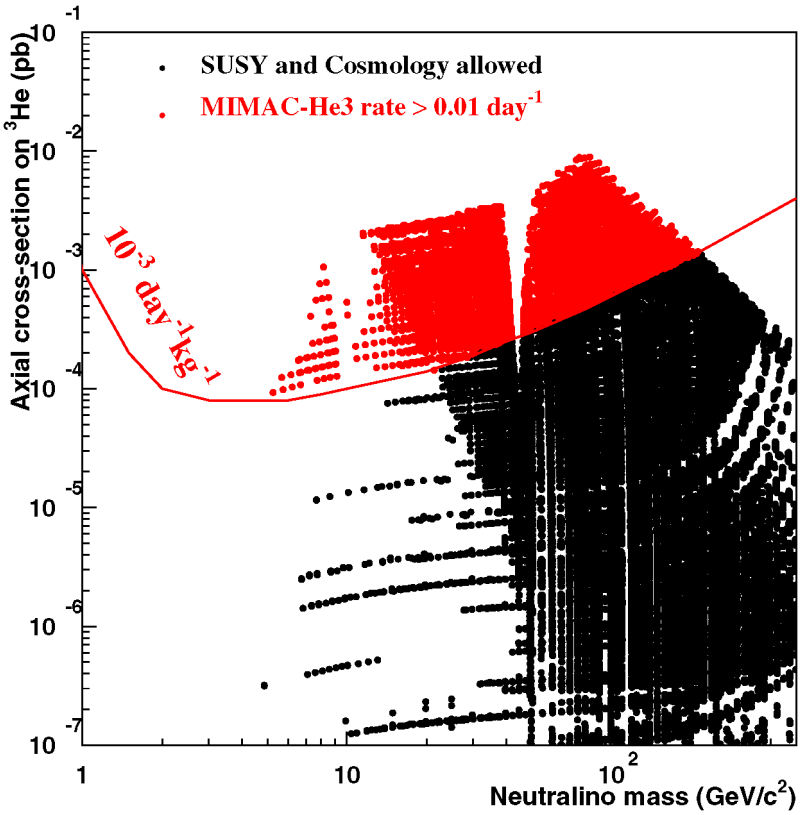

Fig. 1. Spin-dependent cross-section on ^{3}He (pb) versus the neutralino mass (GeV/c^2). Black points correspond to SUSY models allowed by collider and cosmological constraints ($\sim 4 \times 10^5$ models). Projected exclusion curve for MIMAC-He3 (red solid line) with 10^{-3} day^{-1} kg^{-1} background level is drawn. Models accessible by MIMAC-He3 correspond to red points ($\sim 1.7 \times 10^5$ models). (For interpretation of the references to colour in this figure legend, the reader is referred to the web version of this Letter.)

and providing a $\tilde{\chi}$ relic density in the range of interest (Section 3.3.2) leading to $\sim 4 \times 10^5$ allowed models for our scan. The projected exclusion curve for MIMAC-He3 corresponding to a 10^{-3} day^{-1} kg^{-1} background [12] level is drawn.

The very low energy threshold (~ 1 keV) [12] allows to be sensitive to light neutralinos $\tilde{\chi}$ down to ~ 6 GeV/c^2 masses. Models giving a neutralino rate higher than the expected background are selected (above the exclusion curve), hereafter referred to as *accessible* to MIMAC-He3. They correspond to $\sim 1.7 \times 10^5$ models. It can be noticed that MIMAC-He3 would present a sensitivity for neutralino masses from ~ 6 to 200 GeV/c^2 for the expected background level.

When the $\tilde{\chi}$ mass approaches 40 GeV/c^2, the spin-dependent cross-section on ^{3}He suddenly decreases. Indeed, the mass $M_Z/2$ represents a resonance in the annihilation cross-section thus leading to a decrease in $\Omega_{\tilde{\chi}}$. The neutralinos associated to such models provide a relic density $\Omega_{\tilde{\chi}}$ lower than 0.02. The maximum cross-section is $\sim 10^{-2}$ pb for $\tilde{\chi}$ mass ~ 90 GeV/c^2 and it decreases with increasing masses.

4.2. Complementarity with existing scalar detectors

We study here the complementarity between the axial and the scalar interactions, the latter one being widely exploited by most of the ongoing detectors. In order to compare the potentiality of MIMAC-He3 with respect to scalar detectors, the accessible models are distributed in the scalar cross-section on proton versus neutralino mass plane. Within the framework described in Section 3.2, the scalar cross-section on

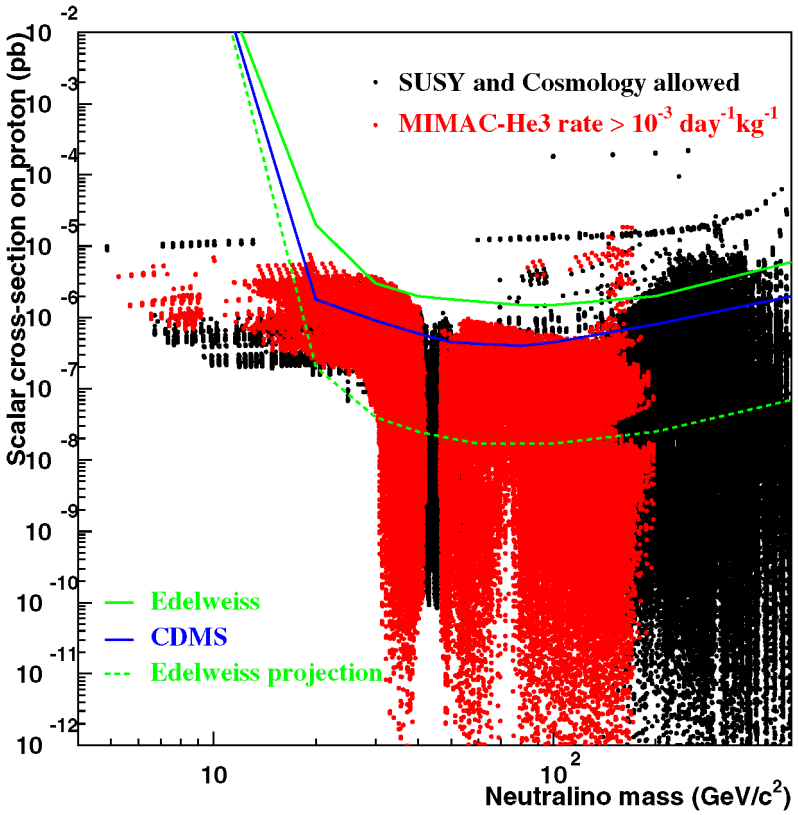

Fig. 2. Scalar cross-section on proton (pb) versus the neutralino mass (GeV/c^2). Black points region represent supersymmetric models satisfying both collider and cosmological constraints. The models accessible by MIMAC-He3 correspond to red points. Exclusion curves from CDMS [8] and Edelweiss [7] experiments are plotted as well as the projected limit for Edelweiss (dotted line). (For interpretation of the references to colour in this figure legend, the reader is referred to the web version of this Letter.)

proton has been evaluated in the whole SUSY parameter space. Fig. 2 presents the scalar cross-section on proton versus the $\tilde{\chi}$ mass for SUSY models satisfying both collider and cosmological constraints. An horizontal branch is observed towards light $\tilde{\chi}$ masses corresponding to scalar cross-sections up to 10^{-5} pb. Models providing smaller cross-sections imply too small values of $\Omega_{\tilde{\chi}}$.

Exclusion curves from ongoing detectors have been plotted [7,8]. Models accessible to MIMAC-He3 have been projected in this diagram and it can be seen how they are distributed. First, it can be noticed that SD and SI cross-section values can be extremely different. Some SUSY models lie below the limits from scalar detectors (CDMS, Edelweiss) whereas they provide a $\tilde{\chi}$ event rate in MIMAC-He3 higher than its background level. On the other hand, for such detectors, the energy threshold arises around 20 GeV/c^2 leading to a significant loss in sensitivity for WIMP masses below. A large part of light $\tilde{\chi}$, below 20 GeV/c^2, escapes from CDMS and Edelweiss detection whereas such a population is accessible to MIMAC-He3. Projected exclusion curves are also presented. Models visible by MIMAC-He3 remain unreachable even for large mass detectors. This point highlights the complementarity between SD and SI direct dark matter detection.

4.3. Complementarity with indirect detection

Indirect detection techniques are based on the measurement of particle flux (e^+, γ, $\bar{p}$, $\bar{D}$, ν) induced by pair annihilation of neutralinos. For instance, neutralinos can be captured gravitationally in celestial objects such as the Sun or the Earth and can annihilate in

high energetic neutrinos [6]. Earth signals are expected to be correlated to scalar direct detection due to the presence of even–even nuclei entering in Earth composition whereas signals from the Sun being made of both odd and even nuclei (H, He) should be correlated to axial and scalar direct detections. In the theoretical framework described above (Section 3.2), the possible complementarity of MIMAC-He3 with neutrino telescopes such as ANTARES [25] or IceCube [26] is investigated.

The results are presented in terms of upward muon fluxes above an energy threshold of 1 GeV [25] which will be the threshold of the next generation of the km^2-size neutrino telescopes. Fig. 3 shows the muon flux coming from the Sun (km^{-2} year^{-1}) versus the $\tilde{\chi}$ rate in MIMAC-He3 (day^{-1}), for a 10 kg detector. The background for the neutrino telescopes is given by cosmic rays interacting in the Sun's corona. It is usually taken at 10 km^{-2} year^{-1} [27]. As a comparison, latest Super-Kamiokande results on WIMP-induced upward muon flux from Sun [28] (for a 50 GeV/c^2 WIMP) is of the order of 1.6×10^3 km^{-2} year^{-1}, but with an energy threshold of 18 GeV/c^2. In the case of MIMAC-He3, the background level is considered at 10^{-3} day^{-1} kg^{-1}. Four regions can be separated in this figure. First, some models lie below the 2 expected background levels: they are not accessible. On the contrary, models in the upper right part of the figure should be seen via both detection methods. Light neutralinos are expected to be visible only in MIMAC-He3 because they yield a muon flux well below the background level.

4.4. Complementarity with spin-dependent direct detection experiments

In the case of the SI interaction, the limits on the cross-section on the nucleus can be translated to bounds on the WIMP-proton cross-section. The conversion is relatively straightforward given the fact that the WIMP coupling to the nucleus is proportional to the square of the nucleus mass. The comparison of experimental results concerning the SD interaction is more problematic. Since the spin of the target nucleus is carried both by constituent protons and neutrons, when converting to a WIMP-proton cross-section a value of the ratio of the WIMP-proton and WIMP-neutron cross-sections must be assumed. But this ratio can vary significantly depending on the WIMP composition. Recently, a model-independent method [29] has been developed to enable comparison among SD direct searches of dark matter. The WIMP-nucleon cross-sections $\sigma_{p,n}^{\lim(A)}$ are given by [29], in the limit $a_n = 0$ (respectively $a_p = 0$)

$$\sigma_{p,n}^{\lim(A)} = \frac{3}{4}\frac{J}{J+1}\frac{\mu_{p,n}^2}{\mu_A^2}\frac{\sigma_A}{\langle S_{p,n}\rangle^2}, \tag{4}$$

where $\mu_{p,n}^2$ is the WIMP-proton (respectively neutron) reduced mass and σ_A the WIMP-nucleus cross-section limit deduced from experiment.

As shown in [29], the allowed values of $a_{p,n}$, for a given WIMP mass, are required to fall in the inside region defined by

$$a_p \leqslant -\frac{\langle S_n\rangle}{\langle S_p\rangle}a_n \pm \sqrt{\frac{\pi}{24G_F^2\mu_p^2}\sigma_p^{\lim(A)}}. \tag{5}$$

In such a framework, exclusion curves are presented in the (a_p, a_n) plane for a given WIMP mass $M_{\tilde{\chi}}$, where a_p and a_n are respectively the effective proton and neutron coupling strengths. Consistent exclusion curves are 3-dimensional plot: a_p, a_n and $M_{\tilde{\chi}}$. For detectors with one active nucleus, they are composed of two straight lines for which the gradient is given by the ratio $-\langle S_n\rangle/\langle S_p\rangle$. Allowed values of a_p and a_n lie in between these two straight lines. Consequently, the values of the spin contents of target nuclei are a key point for SD detection. Commonly used values are recalled in Table 2 for the reader's convenience.

Fig. 4 shows exclusion curves for ongoing spin-dependent searches in the (a_p, a_n) plane for selected 20 (left side) and 50 GeV/c^2 (right side) WIMP masses: CRESST-^{27}Al [9] (dashed line), Edelweiss-^{73}Ge [31] (dash-dotted line), SIMPLE-^{19}F [32] (dotted line) and ZEPLIN-I-^{129}Xe [33] (yellow solid line).

Table 2
Proton and neutron spin content values for various nuclei. Values are taken from [29] and the references therein. For discussions, see [30]

Nucleus	$\langle S_p\rangle$	$\langle S_n\rangle$
^{3}He	−0.050	**0.490**
^{19}F	**0.477**	−0.004
^{27}Al	**0.343**	0.030
^{73}Ge	0.030	**0.378**
^{129}Xe	0.028	**0.359**

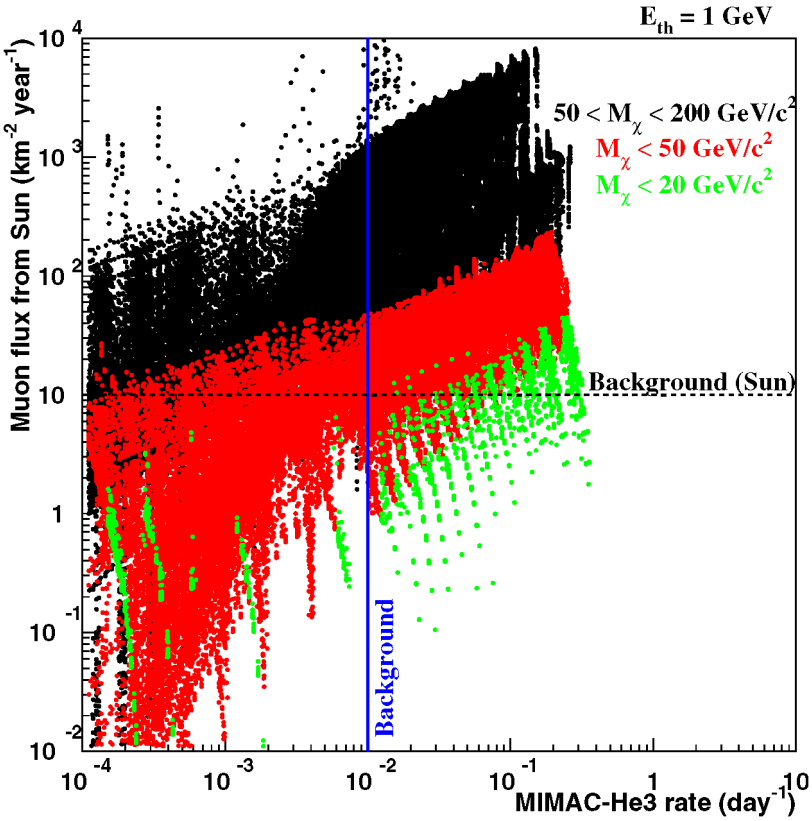

Fig. 3. WIMP-induced upward muon flux from Sun ($\mathrm{km}^{-2}\ \mathrm{year}^{-1}$) versus the $\tilde{\chi}$ rate in MIMAC-He3 (day^{-1}) for different $\tilde{\chi}$ mass ranges. The muon energy threshold is 1 GeV. Background from energetic neutrinos produced in Sun's corona [27] (dashed line) and expected background for MIMAC-He3 (solid lines) is indicated.

In the upside plots, the current excluded region (dark gray) is defined, for each WIMP mass, by the intersection of the most constraining exclusion curves. It should be noticed that in the 20 GeV/c^2 mass case, Edelweiss constraint does not appear in this (a_p, a_n) range. The MIMAC-He3 projection (red solid line) allows to further constrain the current allowed region leading to a projected excluded region defined by the light gray region. Only the white region should be left allowed with MIMAC-He3. The downside plots present a zoom for WIMP masses of 20 and 50 GeV/c^2. It can be seen that MIMAC-He3 should allow to put much stronger constraints on the SUSY region, especially for light WIMP masses for which other neutron based detectors provide much weaker constraints, due to threshold and target nucleus mass effects.

In addition to be a model-independent framework, the (a_p, a_n) diagram highlights the natural complementarity between various SD detectors. In particular, proton based (^{19}F, ^{23}Na, ^{27}Al, ^{35}Cl, ^{127}I) and neutron based detectors (^{3}He, ^{73}Ge, ^{129}Xe) provide orthogonal constraints. Furthermore, the sign of the $\langle S_n\rangle/\langle S_p\rangle$ ratio governs the sign of the slope thus giving another complementarity among neutron based detectors.

However, due to the wide range for a_p and a_n, between experimental constraints and expected SUSY models, a more convenient representation would be obtained in the nucleon SD cross-section plane (σ_p, σ_n). Two cases should then be distinguished depending on the sign of the ratio $\langle S_p\rangle a_p/\langle S_n\rangle a_n$: the constructive (positive sign) or the destructive (negative sign) interferences.

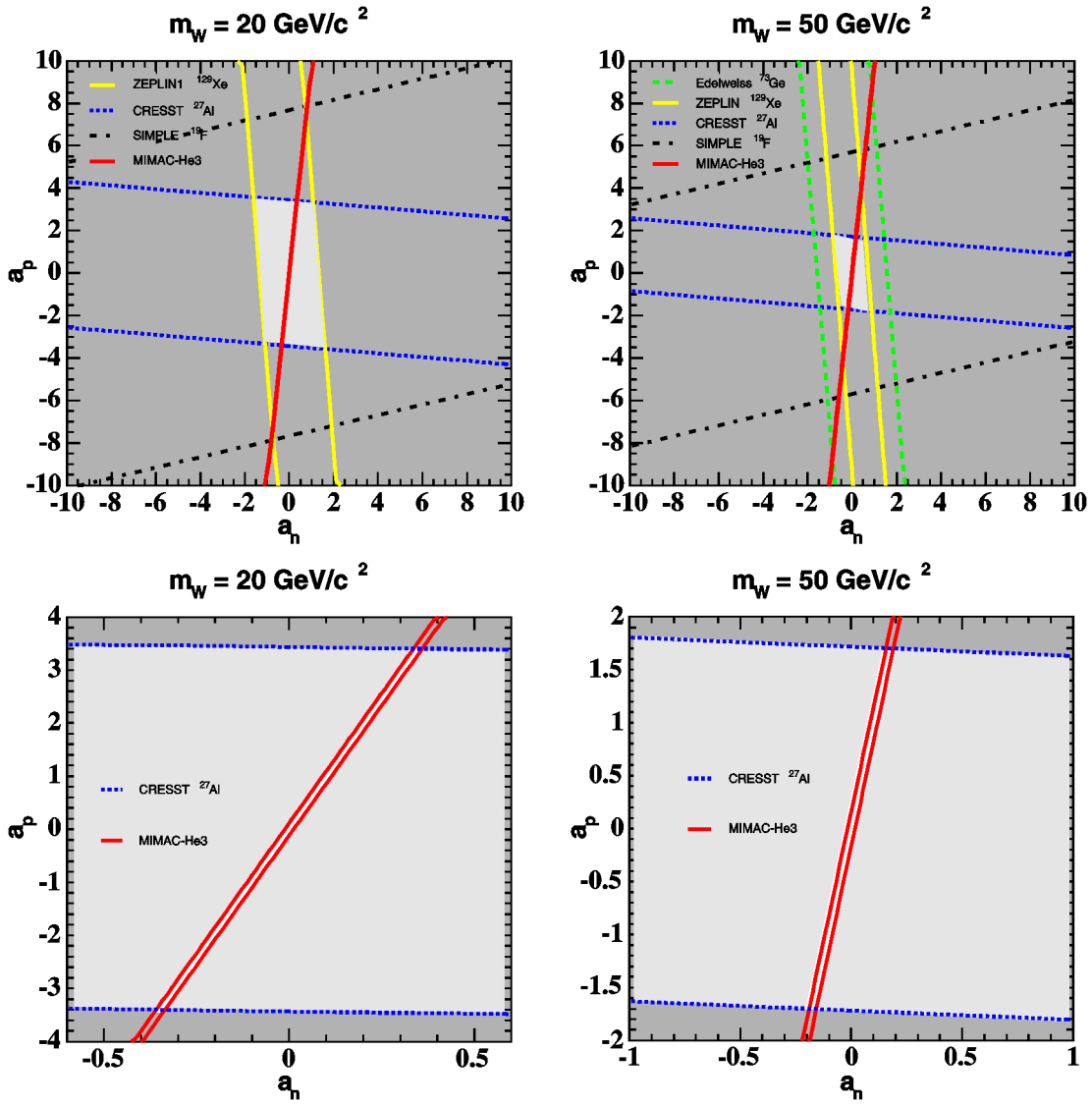

Fig. 4. Exclusion curves for spin-dependent direct dark matter searches in the (a_p, a_n) plane. The exclusion curves from CRESST-^{27}Al [9] (dashed line), Edelweiss-^{73}Ge [31] (dash-dotted line), SIMPLE-^{19}F [32] (dotted line) and ZEPLIN-I-^{129}Xe [33] are plotted. In the upside plots, the current excluded regions (dark gray) are defined by the intersection of the most constraining exclusion curves (ZEPLIN-I and CRESST). The MIMAC-He3 projection (red solid line) allows to further constrain this region leading to a projected excluded region defined by the light gray region. Only the white region should be left allowed with MIMAC-He3. The downside plots present a zoom for WIMP masses of 20 GeV/c^2 (left) and 50 GeV/c^2 (right). (For interpretation of the references to colour in this figure legend, the reader is referred to the web version of this Letter.)

Fig. 5 shows the result in the (σ_p, σ_n) plane in the destructive (left side) and constructive (right side) interference cases, for 20 GeV/c^2 (upper side) and 50 GeV/c^2 (down side) neutralinos. For a given exclusion limit, the excluded region lies outside the two curves. First, it should be noticed that, for a given experiment, there is a rather large difference between the two types of interferences in terms of experimental constraints. Indeed, in the destructive case, some models with both high neutron and pro-

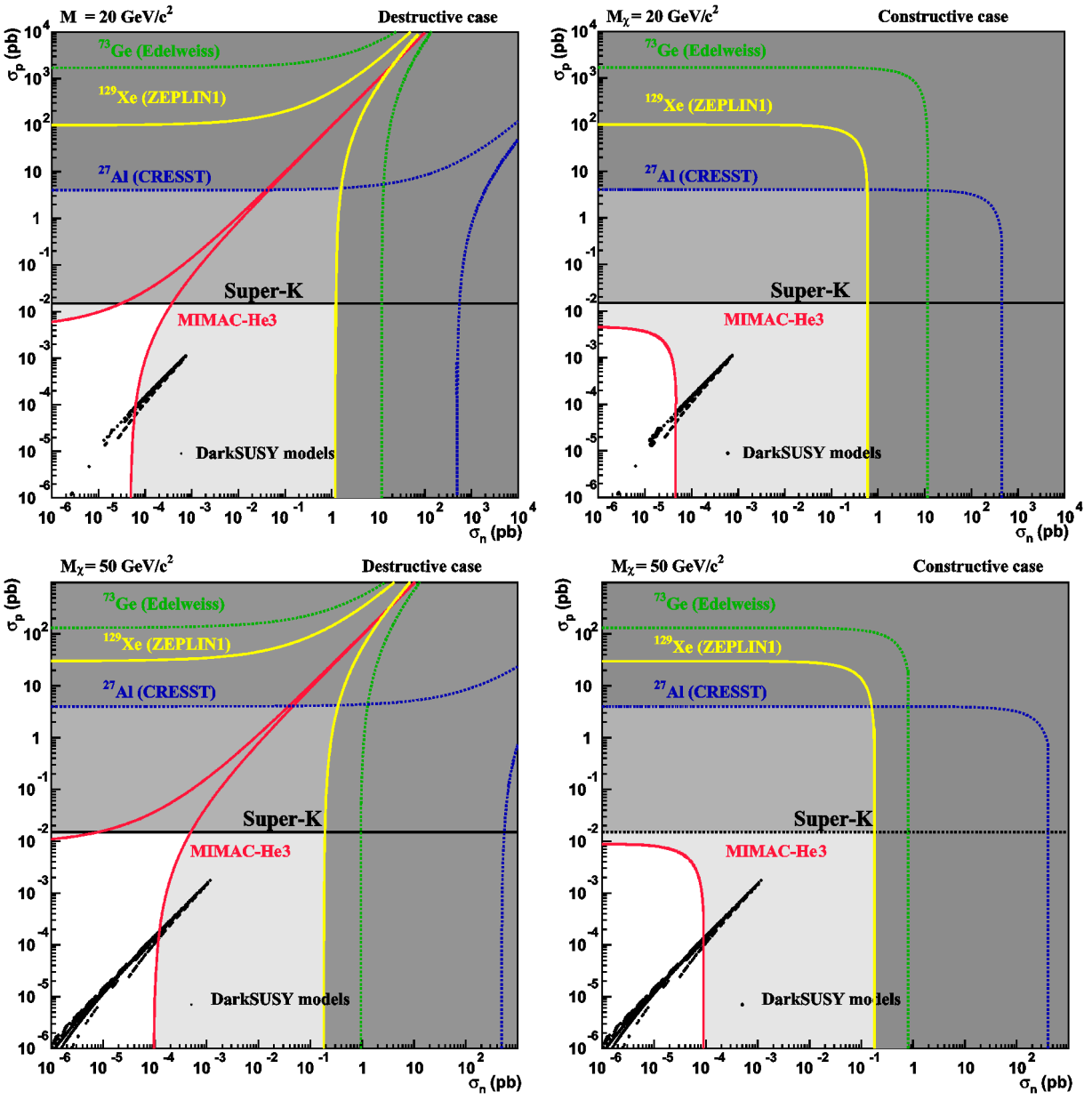

Fig. 5. SUSY models satisfying both accelerator and cosmological constraints (black points) are presented in the cross-section on proton (pb) versus cross-section on neutron (pb) diagram for 20 GeV/c^2 (upper plots) and 50 GeV/c^2 (lower plots) neutralino masses in the case of destructive interferences (left side plots) and constructive interferences (right side plots). The projection exclusion curve of MIMAC-He3 corresponds to the red solid line. Exclusion curves from Edelweiss-^{73}Ge (dashed line), CRESST-^{27}Al (dotted line) and ZEPLIN-I-^{129}Xe [9,31,33] are plotted. The limit from Super-K [28] is also displayed (solid black line). Dark gray corresponds to region currently excluded by SD direct detection, medium gray when adding the Super-K constraint and light gray with projected MIMAC-He3 exclusion. (For interpretation of the references to colour in this figure legend, the reader is referred to the web version of this Letter.)

ton cross-sections may still remain unreachable to a given target nucleus, i.e., models lying inside the "funnel".

Several exclusion curves are presented on Fig. 5, such as CRESST (dotted line), ZEPLIN-I (yellow solid line) and Edelweiss (dashed line). These curves are obtained from calculation based on [9,31].

The current excluded region (light gray) in this plane is given by the combination of theses curves. It also includes the limit from indirect DM detection (ν telescopes). As said previously, the capture rate in the Sun and thus the neutrino flux is exclusively sensitive to the SD cross-section on proton. Therefore, a band along the σ_n axis is obtained. The Super-K limit (black solid line) is displayed [28] on Fig. 5. The constraint from this experiment strongly reduces the allowed region. A near orthogonality is obtained with neutron based experiments. On the other hand, proton based experiments (CRESST) are well overlapped by Super-K limit.

However, SUSY models (black points) neither excluded by accelerator nor cosmological constraints lie well below this limit. All the models from a large SUSY parameter scan including non-universal models, correspond to higgsino-like neutralinos for which a_p/a_n is of the order of 1.5. In the case of gaugino neutralinos, this ratio can vary by several orders of magnitude as demonstrated in [34].

The projected exclusion curve for MIMAC-He3 is displayed, showing a strong constraint on the SD cross-section on neutron. It can be seen that most of $20\ \mathrm{GeV}/c^2$ neutralinos, escaping from detection of ongoing experiments, would be visible by MIMAC-He3. A large part of $50\ \mathrm{GeV}/c^2$ neutralinos would also be accessible. In conclusion, MIMAC-He3 would present a sensitivity to SUSY models allowed by present cosmology and accelerator constraints. This study highlights the complementarity of this experiment with most of current SD experiments: proton based detectors as well as ν telescopes.

5. Conclusion

It has been shown that a 10 kg ^{3}He detector with a threshold of about 1 keV and with electron-recoil discrimination (MIMAC-He3) would allow to reach in a significant part of the SUSY parameter space, a $\tilde{\chi}$ event rate higher than the estimated background. MIMAC-He3 would be sensitive to SUSY models excluded neither by collider limits nor by neutralino relic density constraint. This new project would be sensitive to SUSY regions not accessible by ongoing scalar detectors. The complementarity of MIMAC-He3 with ongoing experiments is due to its sensitivity to spin-dependent interaction and its light target nucleus allowing to detect light neutralinos which are out of reach of existing detectors.

Acknowledgement

The authors wish to thank M. Bastero-Gil for fruitful discussions.

References

[1] D. Spergel, et al., Astrophys. J. Suppl. 148 (2003) 175.
[2] A. Benoît, et al., Astron. Astrophys. 399 (2003) L25.
[3] S. Perlmutter, et al., Phys. Rev. Lett. 83 (1999) 670.
[4] M. Tegmark, et al., Astrophys. J. 606 (2004) 702.
[5] S. Eidelman, et al., Phys. Lett. B 592 (2004) 1.
[6] G. Jungman, et al., Phys. Rep. 267 (1996) 195.
[7] A. Benoît, et al., Phys. Lett. B 545 (2002) 43.
[8] D. Akerib, et al., Phys. Rev. Lett. 93 (2004) 211301.
[9] W. Seidel, et al., in: H.-V. Klapdor-Kleingrothaus, et al. (Eds.), Proceedings of the 4th International Conference on Dark Matter in Astro and Particle Physics (DARK 2002), Cape Town, South Africa, February 2002, Springer, Berlin, 2002.
[10] E. Moulin, et al., Nucl. Instrum. Methods A, submitted for publication.
[11] D. Santos, E. Moulin, astro-ph/0412273, in: Proceedings of the 5th International Workshop on the Identification of Dark Matter (IDM 2004), Edinburgh, Scotland, September 2004, in press.
[12] D. Santos, E. Moulin, et al., in preparation.
[13] D. Santos, et al., in: D.B. Cline (Ed.), Proceedings of the 4th International Symposium on Sources and Detection of Dark Matter and Dark Energy in the Universe (DARK 2000), Marina Del Rey, CA, USA, February 2000, Springer, New York, 2000, p. 469, astro-ph/0005332.
[14] F. Mayet, et al., Nucl. Instrum. Methods A 455 (2000) 554.
[15] E. Moulin, et al., in: V. Le Brun, et al. (Eds.), Proceedings of the 4th International Marseille Cosmology Conference, Where Cosmology and Fundamental Physics Meet, Marseille, France, June 2003, Frontier Group, 2003, p. 161, astro-ph/0309325.
[16] V. Kudryavtsev, et al., Nucl. Instrum. Methods A 505 (2003) 688.
[17] F. Mayet, et al., Phys. Lett. B 538 (2002) 257.
[18] J. Ellis, et al., Phys. Lett. B 155 (1985) 381;

M. Drees, et al., Phys. Lett. B 158 (1985) 409;
M. Drees, et al., Phys. Rev. D 33 (1986) 1486.
[19] D. Hooper, et al., Phys. Lett. B 562 (2003) 18.
[20] A. Bottino, et al., Phys. Rev. D 67 (2003) 063519.
[21] G. Bélanger, et al., JHEP 0403 (2004) 012.
[22] P. Gondolo, et al., JCAP 0407 (2004) 008.
[23] G. Bélanger, et al., hep-ph/0502079.
[24] L. Bergström, et al., Phys. Rev. D 59 (1999) 043506.
[25] ANTARES Collaboration, B. Vallage, in: Proceedings of the 13th International Symposium on Very High Energy Cosmic Ray Interactions, Pylos, Greece, September 2004, in press.
[26] IceCube Collaboration, S. Yoshida, in: Proceedings of the 8th International Workshop on Topics in Astroparticle and Underground Physics, Seattle, USA, September 2003, in press.
[27] D. Seckel, et al., Astrophys. J. 382 (1991) 652.
[28] S. Desai, et al., Phys. Rev. D 70 (2004) 109901.
[29] D. Tovey, et al., Phys. Lett. B 488 (2000) 17.
[30] V. Bednyakov, et al., hep-ph/0406218.
[31] A. Benoit, et al., astro-ph/0412061.
[32] J. Collar, et al., Phys. Rev. Lett. 85 (2000) 3083.
[33] V. Kudryavtsev, et al., in: Proceedings of the 5th International Workshop on the Identification of Dark Matter (IDM 2004), Edinburgh, Scotland, September 2004, in press.
[34] J. Lewin, et al., Astropart. Phys. B 6 (1996) 87.